

# Chaotic Oscillations of Nonideal Plane Pendulum Systems

Aleksandr Yu. Shvets<sup>1</sup> and Alexander M. Makaseyev<sup>2</sup>

<sup>1</sup> National Technical University of Ukraine “Kyiv Polytechnic Institute”,  
Kyiv, Ukraine (E-mail: [alex.shvets@bigmir.net](mailto:alex.shvets@bigmir.net))

<sup>2</sup> National Technical University of Ukraine “Kyiv Polytechnic Institute”,  
Kyiv, Ukraine (E-mail: [makaseyev@ukr.net](mailto:makaseyev@ukr.net))

**Abstract.** The atlas of maps of dynamic regimes of system “pendulum–electric motor” is constructed. It is established that the deterministic chaos is a typical steady-state regime of the given system. Its class of Feigenbaum universality is defined. The analytical approximation of a Poincare map in a chaotic regime is discovered.

**Keywords:** nonideal systems, chaotic attractors, Feigenbaum constant, Poincare maps.

## 1 Introduction

In the majority of investigations of the dynamics of pendulum systems are being conducted without taking into account the limitations of excitation source power, so it is assumed that the power of excitation source considerably exceeds the power that the vibrating system consumes. Such systems are called ideal in sense of Sommerfeld–Kononenko [2]. In many cases such idealization leads to qualitative and quantitative errors in describing dynamical regimes of pendulum systems [4]–[6].

Therefore, in most practical problems an object “the oscillating system – the source of oscillation” should be principally treated as a nonideal in sense of Sommerfeld–Kononenko dynamical system [2]. In such systems, the oscillation source power is always assumed comparable to the power consumed by the oscillating system. This requires taking into account interactions between oscillating loading and the energy source of oscillations.

## 2 Mathematical model of the system

As it has been established in [4]–[6], the motion equations of the “pendulum–electric motor” can be described by the following deterministic dynamical system:



$$\begin{aligned}
\frac{dy_1}{d\tau} &= Cy_1 - y_2y_3 - \frac{1}{8}(y_1^2y_2 + y_2^3); \\
\frac{dy_2}{d\tau} &= Cy_2 + y_1y_3 + \frac{1}{8}(y_1^3 + y_1y_2^2); \\
\frac{dy_3}{d\tau} &= Dy_2 + Ey_3 + F;
\end{aligned} \tag{1}$$

where phase variables  $y_1y_2$  describe the pendulum deviation from the vertical and phase variable  $y_3$  is proportional to the rotation speed of the motor shaft. The system parameters are defined by

$$C = -\frac{\delta}{\omega_0} \left(\frac{a}{l}\right)^{-2/3}, D = -\frac{2ml^2}{I}, F = 2\left(\frac{a}{l}\right)^{-2/3} \left(\frac{N_0}{\omega_0} + E\right) \tag{2}$$

where  $m$  - the pendulum mass,  $l$  - the reduced pendulum length,  $\omega_0$  - eigenfrequency of the pendulum,  $a$  - the length of the electric motor crank,  $\delta$  - damping coefficient of the medium resistance force,  $I$  - the electric motor moment of inertia,  $E, N_0$  - constants of the electric motor static characteristics.

Since the system of equations (1) is nonlinear, the identification and study of its attractors can only be done through a series of numerical methods and algorithms. The methodology of such studies is suggested and described in [6], [7].

### 3 Maps of dynamic regimes

A very clear picture of the dynamical system behavior can give us a map of dynamic regimes. It is a diagram on the plane, where two parameters are plotted on axes and the boundaries of different dynamical regimes areas are shown. Since the number of parameters in the system (1) is more than two, the detailed map of dynamic regimes will consist of many sheets.

In fig. 1 several sheets of dynamical regimes maps are shown. Two of four parameters ( $C, D, E, F$ ) of the system (1) were constants and two others varied within certain limits. The map in fig. 1a was built when  $C = -0.1, E = -0.59$ . The map in fig. 1b was built when  $F = -0.17, E = -0.59$ . The last two maps in fig. 1c-d were built when  $D = -0.6, F = 0.19$  and  $C = -0.1, F = 0.19$  respectively. The dark-grey areas of the maps correspond equilibrium positions of the system (1), the light-grey - to limit cycles and the black - to chaotic attractors.

As we can see, in each map there are extensive areas where the system has chaotic regimes. This means that the deterministic chaos is a typical steady-state regime of the given system.

It should be emphasized that consideration the problem in ideal formulation, i.e. neglecting the pendulum influence on electric motor functioning, can lead to gross errors in describing of the dynamics of system. Indeed, in the ideal formulation of the problem in the system of equations (1) should be put  $D = 0$ , then the system of equations disintegrates into two subsystems. The first one

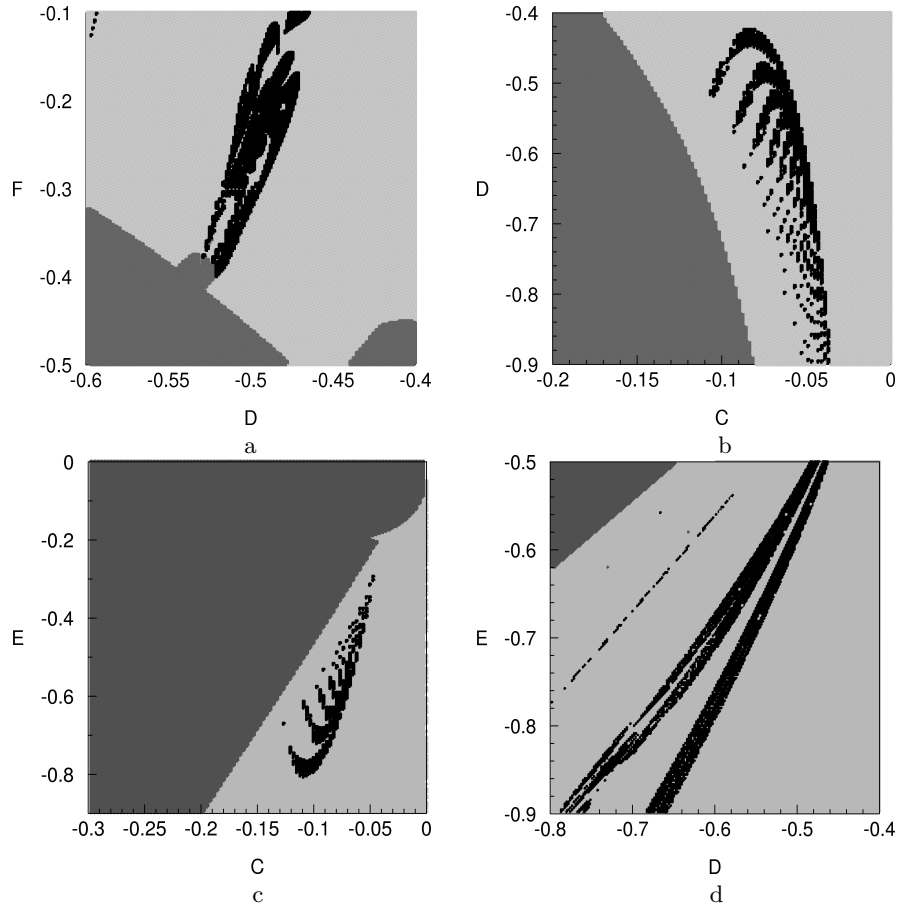


Fig. 1. Maps of dynamic regimes

will consist of the first two equations of (1), and the second one will consist of the one third equation of the system (1). Therefore, in the ideal formulation of the problem, the maximum phase space dimension of the obtained equations will be equal to two. In the spaces of this dimension the existence of chaotic attractors is theoretically impossible [6], [1].

The obtained maps of dynamical regimes allow us to conduct a quick qualitative identification of the type of steady-state regime of the system (1). On the basis of the constructed maps, more detailed studies of emerging dynamic regimes can be carried out. Particularly, the transition from regular to chaotic regimes.

For this purpose, we carry out a vertical (horizontal) section of maps and build other characteristics of the system. For instance, let us carry out a vertical section of the map, that is shown in fig. 1b, along the line  $C = -0.07$ . In fig 2a a fragment of phase-parametric characteristic ("bifurcation tree") of the system is shown and in fig 2b the dependence of maximal non-zero Lyapunov's characteristic exponent of the system from the parameter  $F$  is

depicted. These characteristics correspond to the parameter  $D$  change in range of  $-0.55$  to  $-0.4$ . The intervals of the parameter  $D$ , in which there are separate branches of the bifurcation tree "crown", correspond to the periodic regimes of the system steady oscillations. And the intervals in which the "crown" is represented by saturated black color, correspond to chaotic regimes. As it has been established in [4]–[6], this kind of "bifurcation tree" corresponds to transitions "cycle – chaos" according to the Feigenbaum's scenario from the right side of the bifurcation parameter changes and to intermittency in the sense of Pomeau-Manneville from the left side of the bifurcation parameter changes.

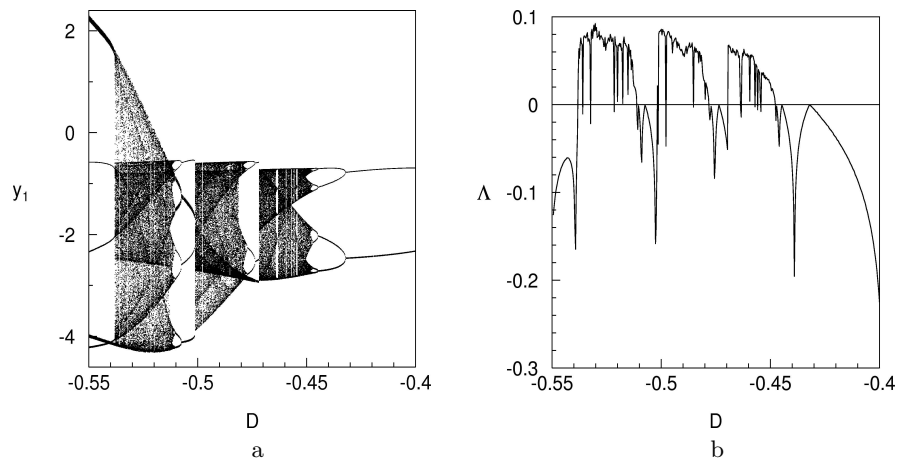


**Fig. 2.** Phase-parametric characteristic of the system (a), the dependence of maximal non-zero Lyapunov's characteristic exponent (b)

#### 4 The universality class determination

Let us consider the behavior of the system when parameters are  $C = -0.1$ ,  $D = -0.5$ ,  $E = -0.59$ , and  $0.16 \leq F \leq 0.27$ . In fig. 3a the dependence of maximal non-zero Lyapunov's characteristic exponent of the system (1) from the parameter  $F$  is depicted. As we can see, there are several intervals of variation  $F$  where the system has positive Lyapunov's characteristic exponent. The attractor of the system in these intervals is a chaotic attractor. In the region of existence of chaotic attractors, in the left side of the fig. 3a, we can notice several dips of the Lyapunov's exponent graph to negative values. Small intervals of the parameter  $F$  in which there are such dips form the so-called windows of periodicity in chaos. In these windows attractors of the systems are limit cycles. Also in the right side of the fig. 3a we can clearly see the approaches of maximal Lyapunov's exponent to the zero line, which correspond to the points of bifurcation of period-doubling.

In fig. 3b the phase-parametric characteristic of the system is shown. A close examination of this figure shows as the bifurcation points of regular

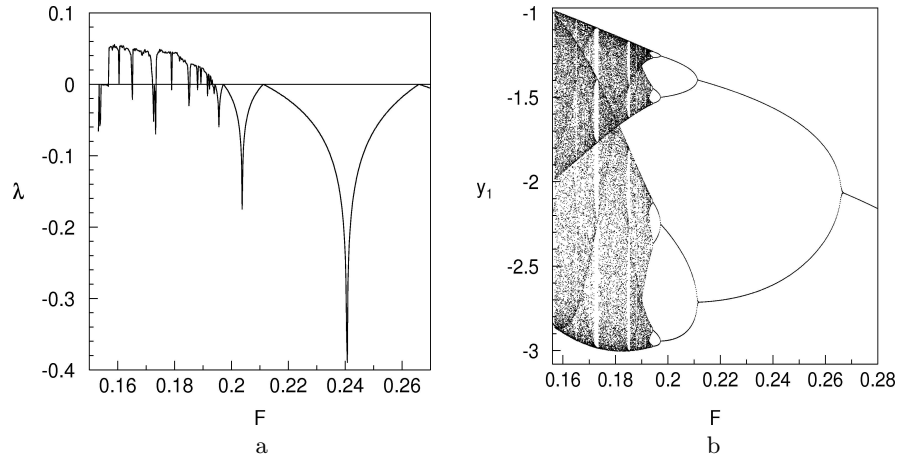


**Fig. 3.** The dependence of maximal non-zero Lyapunov's characteristic exponent from  $F$  (a), phase-parametric characteristic of the system (b).

regimes as well as the bifurcation points, at passing of which, regime changes from regular periodic to chaotic. So in this case, at decreasing the parameter  $F$ , transition to chaos happens through the infinite cascade of period-doubling bifurcations according to the Feigenbaum's scenario.

In order to determine the class of universality for the system (1), we need to calculate the Feigenbaum's constant, which is determined by the formula:

$$\delta = \lim_{n \rightarrow \infty} \delta_n = \lim_{n \rightarrow \infty} \frac{F_n - F_{n-1}}{F_{n+1} - F_n}, \quad (3)$$

where  $F_n$  – value of the bifurcation parameter at the  $n$ -th point of period-doubling bifurcation.

Bifurcation values of  $F_n$  correspond to the approaches of maximal Lyapunov's exponent to the zero line (fig. 3a) or to the cleavage points of separate branches of "bifurcation tree" in fig. 3b. We should mention, that for a correct calculation of the Feigenbaum's constant the bifurcation values of  $F_n$  must be determined with a sufficiently high accuracy. Therefore using fig. 3 we initially roughly define the interval of the parameter  $F$  variation that contains the first bifurcation point. As can be seen from fig. 3,  $0.26 < F_1 < 0.27$ . Then we build the dependence of maximal Lyapunov's characteristic exponent from  $F$  and phase-parametric characteristic on the interval  $(0.26, 0.27)$  and specify the value of the first bifurcation point. Repeating the procedure of decreasing the interval of the parameter  $F$  variation and constructing the dependence of maximal Lyapunov's characteristic exponent from the parameter  $F$  and phase-parametric characteristic on the smaller scale we can obtain the value  $F_1$  with a sufficiently high accuracy. In order to verify the correctness of the bifurcation point determination we build phase portraits of the system passing the first point of bifurcation and make sure, that the structure of phase portraits changes from single-turn cycle to two-turn cycle. Similar procedures are used for defining the following period doubling bifurcation points.

In our case, the values of bifurcation points were determined with an accuracy to  $\varepsilon < 10^{-7}$ . At  $F = 0.265967$  the attractor of our system is single-turn limit cycle and at  $F = 0.265966$  this cycle loses its stability and in the system arises two-turn limit cycle. We take the average of this two values as the first point of period-doubling bifurcation, so that we assume that  $F_1 = 0.2659665$ . At  $F = 0.211192$  the system has two-turn cycle and at  $F_2 = 0.2111915$  the second period-doubling bifurcation takes place and four-turn cycle arises in the system as a result of it. This cycle loses its stability at  $F_3 = 0.1971565$  and 8-turn limit cycle arises in the system. The fourth and fifth period-doubling bifurcations occur respectively at  $F_4 = 0.1942145$  and  $F_5 = 0.1935835$ . As a result 16- and 32-turn cycles appear in the system. At  $F_6 = 0.1934483$  32-turn limit cycle loses its stability and 64-turn cycle arises in the system. This infinite cascade of period-doubling bifurcations comes to end by origin of a chaotic attractor.

Substituting the obtained values into the formula (3) we get:

$$\delta_2 = 3.90274, \delta_3 = 4.77056, \delta_4 = 4.66244, \delta_5 = 4.66720$$

We take the value  $\delta_5 = 4.66720$  as an approximate value of the Feigenbaum's constant.

Let us show that the value of the Feigenbaum's constant remains virtually unchanged at different set of the parameters of the system (1). Let the parameters of the system are  $C = -0.1$ ,  $D = -0.5$ ,  $F = 0.14$ . As bifurcation parameter we choose  $E$  that varies  $-0.77 \leq E \leq -0.6$ . In fig. 4a,b the dependence of maximal non-zero Lyapunov's characteristic exponent from  $E$  and phase-parametric characteristic of the system are shown respectively.

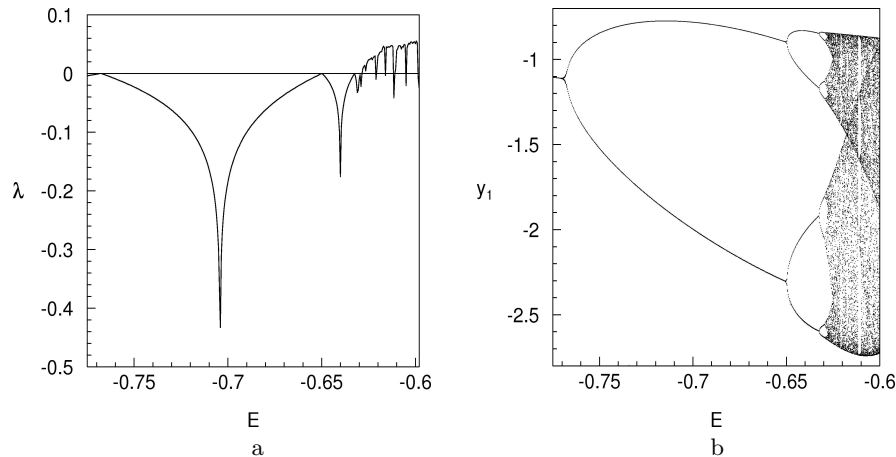


**Fig. 4.** The dependence of maximal non-zero Lyapunov's characteristic exponent from  $E$  (a), phase-parametric characteristic of the system (b).

The qualitative similarity of fig. 3a-b with the respective fig. 4a-b should be noted. As in the previous case, there are several intervals of the parameter change (in this case it is  $E$ ) in which the system has positive Lyapunov's

characteristic exponent (fig. 4a). Therefore in these intervals the system has chaotic attractors. Again in fig. 4a we can clearly see the approaches of maximal Lyapunov's exponent to the zero line. The form of "bifurcation tree" (fig. 4b) clearly illustrates the Feigenbaum's scenario of transition to chaos. However, as opposed to the previous case, the infinite cascade of period-doubling bifurcations takes place at increasing of the bifurcation parameter.

Let us find the values of the parameter  $E$  at which period-doubling bifurcations are happening. The methodology of obtaining these values is similar to that which was used in the previous case for finding bifurcation values of  $F$ . At  $E = -0.76763$  the attractor of our system is single-turn limit cycle, which loses its stability at  $E_1 = -0.767625$  and in the system arises two-turn limit cycle. At  $E = -0.64983$  the system still has two-turn limit cycle and at  $E_2 = -0.649825$  the second period-doubling bifurcation takes place and four-turn cycle arises in the system as a result of it.

This cycle loses its stability at  $E_3 = -0.632405$  and 8-turn limit cycle arises in the system. The fourth and fifth period-doubling bifurcations occur respectively at  $E_4 = -0.629315$  and  $E_5 = -0.628666$ . As a result 16- and 32-turn cycles appear in the system. At  $E_6 = -0.628527$  32-turn limit cycle loses its stability and 64-turn cycle arises in the system. This infinite cascade of period-doubling bifurcations comes to end by origin of a chaotic attractor at  $E = -0.62848$ . Using the formula (3) and respectively substituting the values  $E_i$  instead of  $F_i$  into it, we get the following values:

$$\delta_2 = 6.76234, \delta_3 = 5.63754, \delta_4 = 4.76117, \delta_5 = 4.66906.$$

We take the value  $\delta_5 = 4.66906$  as an approximate value of the Feigenbaum's constant.

The obtained values quite accurately match with the Feigenbaum's constant, which approximately equals 4.6692. This means that we can state that the system (1) apply to class of universality with the classical Feigenbaum's constant.

## 5 Analytical approximation of Poincare map

In the previous studies of the "pendulum–electric motor" [4]–[6] it has been established that chaotic attractors that exist in this system, generally, have "quasi ribbon" type of Poincare maps.

This means that the original system of differential equations can be approximately reduced to one of the discrete maps [3], [1]. The study of the dynamics of this discrete map will be much easier than investigation the dynamics of the original system.

Let the system (1) has following values of parameters  $C = -0.1$ ,  $D = -0.5$ ,  $E = -0.59$ ,  $F = 0.19$ . At these values of the parameters in the system there is a chaotic attractor. Its phase portrait is depicted in fig. 5.

In fig. 6 the Poincare maps of this chaotic attractor are shown. As can be seen from this figure, the Poincare maps on both phase variables have a structure that is close to a line on the plane. Both maps represent some chaotic

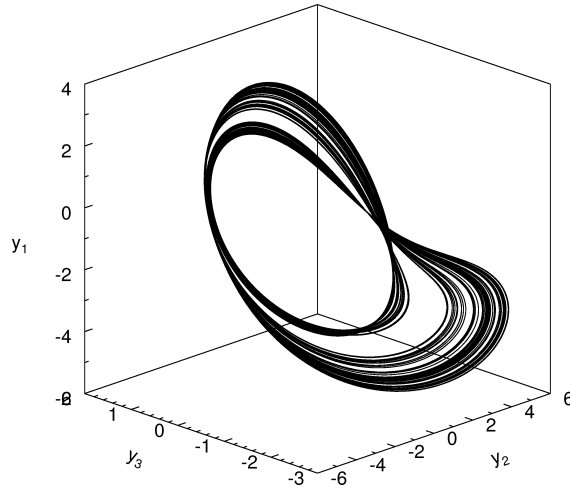


**Fig. 5.** Phase portrait of the chaotic attractor at  $C = -0.1$ ,  $D = -0.5$ ,  $E = -0.59$ ,  $F = 0.19$

set of points. Quantity of these points increases with increasing the time of numerical integration. It is impossible to foresee the order of points placement along "the ribbons" that form the map. However, it is known beforehand that they can only be placed along these ribbons.

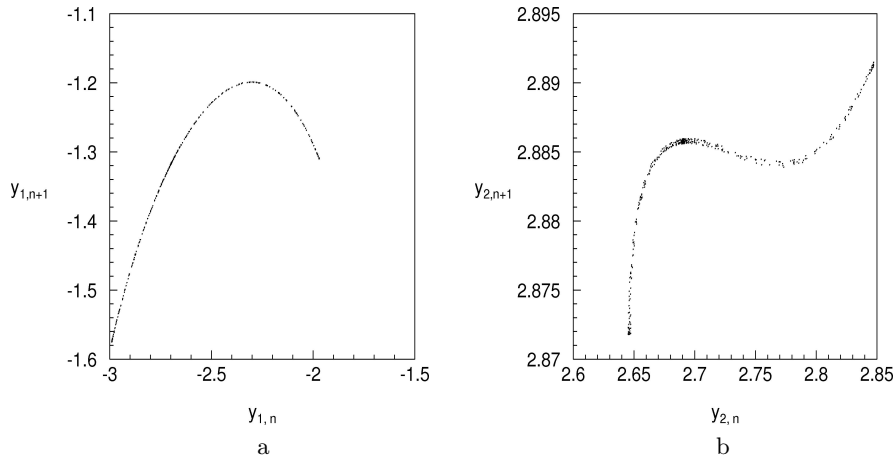


**Fig. 6.** The Poincaré maps of the chaotic attractor.

Let us consider the Poincaré map that is shown in fig. 6a. The graph of this map is defined by a set of discrete coordinate values

$$(y_{1,n+1}, y_{1,n}), \quad n = 1, 2, \dots, N, \tag{4}$$

where  $N$  – is a number of discrete points on which the Poincaré map is constructed. Let us set the problem of finding the polynomial whose graph as close

as possible to the points of the Poincare map. For this purpose, the LS method has been used. For set of points (4) we find a  $m$ -order polynomial:

$$f^{(m)}(y_1) = p_1 y_1^m + p_2 y_1^{m-1} + \dots + p_m y_1 + p_{m+1}, \quad (5)$$

the coefficients of which are solution of the minimization problem

$$\min_{p_1, p_2, \dots, p_{m+1}} \sum_{i=1}^N \left( f^{(m)}(y_{1,i}) - y_{1,i+1} \right)^2. \quad (6)$$

The approximation errors have been estimated using the mean-squared error,

i.e.  $\varepsilon^{(m)} = \sqrt{\min_{p_1, p_2, \dots, p_{m+1}} \sum_{i=1}^N \left( f^{(m)}(y_{1,i}) - y_{1,i+1} \right)^2}$ . Applying this method, the following approximations have been obtained:

$$\begin{aligned} f^{(2)}(y_1) &= -0.8377y_1^2 - 3.8947y_1 - 5.7267, \varepsilon^{(2)} = 0.0506; \\ f^{(3)}(y_1) &= -0.0067y_1^3 - 0.8881y_1^2 - 4.0199y_1 - 5.8292, \varepsilon^{(3)} = 0.0505; \\ f^{(4)}(y_1) &= -0.5365y_1^4 - 5.3596y_1^3 - 20.778y_1^2 - 36.6289y_1 - 25.7282, \\ &\varepsilon^{(4)} = 0.0096. \end{aligned}$$

Then, the only approximation errors are shown:

$$\varepsilon^{(5)} = 0.0087, \varepsilon^{(6)} = 0.0082, \varepsilon^{(7)} = 0.0081, \varepsilon^{(8)} = 0.0081.$$

It is seen that with the increasing the polynomial order, starting from the order  $m = 4$ , the approximation accuracy increases insignificantly.

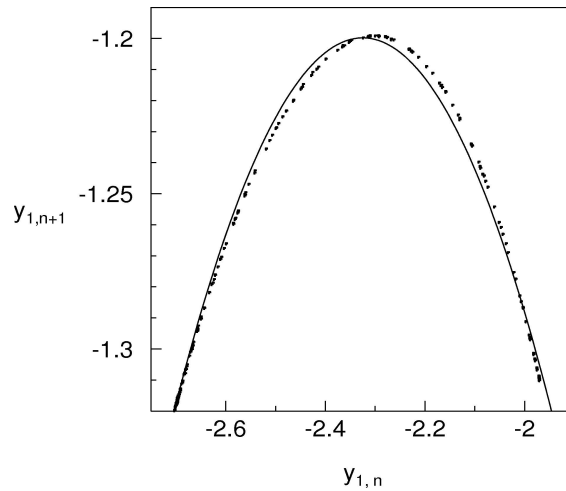


**Fig. 7.** The Poincare map and its second-order polynomial approximation

The fig. 7 shows an enlarged fragment of the constructed polynomial  $f^{(2)}(y_1)$  (continuous line in the figure) that is overlaid on the Poincare map. As can be seen from this figure, these two graphs are close enough to each other. Therefore, this gives us basis to consider the principal possibility to study the continuous system "pendulum–electric motor" (1) using discrete map  $y_{1,n+1} = f^{(2)}(y_{1,n})$ . More accurate results will be obtained when the maps  $y_{1,n+1} = f^{(m)}(y_{1,n})$ ,  $m = 4 \div 8$  are used.

## 6 Conclusion

At the study of the dynamical system "pendulum–electric motor", the atlas of maps of dynamical regimes has been constructed. It has been established that deterministic chaos is a typical steady-state regime of the given system. The Feigenbaum's constant of system "pendulum–electric motor" is obtained. The class of universality of the given system is defined. The analytical polynomial approximations of the Poincare map have been found.

## References

- 1.V. S. Anishchenko, V. V. Astakhov, A. B. Nieman, T. E. Vadivasova, and L. Schimansky Geier. *Nonlinear Dynamics of Chaotic and Stochastic Systems*. Springer, Berlin, 2003.
- 2.V. O. Kononenko. *Vibrating System with a Limited Power-supply*. Iliffe, London, 1969.
- 3.S. P. Kouznetsov. *Dynamic chaos*. Physmatlit, Moscow, 2006, (in russian).
- 4.T. S. Krasnopolskaya, A. Yu. Shvets. Chaotic interactions in a pendulum-energy-source system. *Sov. Appl. Mech.*, vol. 26, 500—504, 1990.
- 5.T. S. Krasnopolskaya, A. Yu. Shvets. Chaos in vibrating systems with limited power-supply. *Chaos*, vol. 3, no. 3, 387—395, 1993.
- 6.T. S. Krasnopolskaya, A. Yu. Shvets. Regular and chaotical dynamics of systems with limited excitation. *R&C Dynamics*, Moscow, 2008, (in russian).
- 7.T. S. Krasnopolskaya, A. Yu. Shvets. Dynamical chaos for a limited power supply oscillations in cylindrical tanks. *Journal of Sound and Vibration*, vol. 322, no. 3, 532—553, 2009.